Journal Name

ARTICLE

The Role of Anions in Adsorbate-induced Anchoring Transitions of Liquid Crystals on Surfaces with Discrete Cation Binding Sites

Received 00th January 20xx,
Accepted 00th January 20xx

DOI: 10.1039/x0xx00000x

www.rsc.org/

Tibor Szilvási,[a,†] Nanqi Bao,[a,†] Huaizhe Yu,[a] Robert J. Twieg,[b] Manos Mavrikakis,[a,*] Nicholas L. Abbott[a,*]

We report a combined theoretical and experimental effort to elucidate systematically for the first time the influence of anions of transition metal salt-decorated surfaces on the orientations of supported films of nematic liquid crystals (LCs) and adsorbate-induced orientational transitions of these LC films. Guided by computational chemistry predictions, we find that nitrate anions weaken the binding of 4′-n-pentyl-4-biphenylcarbonitrile (5CB) to transition metal cations, as compared to perchlorate salts, although binding is still sufficiently strong to induce homeotropic (perpendicular) orientations of 5CB. In addition, we find the orientations of the LC to be correlated across all metal cations investigated by a molecular anchoring energy density that is calculated as the product of the single-site binding energy and metal cation binding site density on the surface. The weaker single-site binding energy caused by nitrate also facilitates competitive binding of adsorbates to the metal cations, leading to more facile orientational transitions induced by adsorbates. Finally, our analysis suggests that nitrate anions recruit water via hydrogen bonding to the metal binding sites, modulating further the relative net binding energies of 5CB and adsorbates to surfaces decorated with metal nitrates. After accounting for the presence of water, we find a universal exponential relationship between the calculated displacement free energies and measured dynamic response of LCs to adsorbates for all metal salts studied, independent of the metal salt anion.

Introduction

Liquid crystals (LCs) are a phase of matter with properties intermediate between crystalline solids and isotropic liquids. The molecules in a LC phase flow in response to shear like a fluid but retain a degree of long-range orientational order akin to a crystalline solid. The preferential orientation of molecules within a LC, termed the director, can be influenced by the introduction of interactions between mesogens (molecules that form LCs) and chemically functionalized interfaces.[1-5] Whereas the majority of past studies of the anchoring of LCs on surfaces involve polymeric surfaces that interact with the LCs via van der Waal's interactions, a distinct class of surfaces that can orient LCs use discrete metal cation binding sites for mesogens. Specifically, coordination interactions between nitrile-containing mesogens (e.g., 4′-pentyl-4-biphenylcarbonitrile, 5CB) and transition metal salts deposited on a surface can be used to achieve surface order and then orientational control of the bulk LC director. Previously, ion induced electric double layers have also been investigated for the orientational control of LCs[6-14] however only coordination interaction can be exploited for the detection of chemical analytes that competitively disrupt the coordination interactions between the metal cation binding sites and LC mesogens.[1,15,16] These LC ordering transitions can be easily transduced by using optical and electrical methods.[2,17,18] Such chemoresponsive LC systems form the basis of a promising approach for detection of a range of targeted chemical species, such as acetone vapor[19], proteins[20-22], lipids[23], organophosphonates (e.g., dimethyl methylphosphonate (DMMP), a nerve agent simulant)[15,16,24-34] etc.

Previous experimental studies have successfully demonstrated surface-driven ordering transitions when DMMP is introduced into a LC film from an adjoining vapor phase. The majority of past studies have focused on high-electron-affinity cations such as Al^{3+}, Fe^{3+}, La^{3+}, Zn^{2+}, or Ni^{2+} coordinated with perchlorate anions.[15,16,25-33] The effect of key design variables, such as identity and surface density of the metal cations on LC anchoring behavior have been elucidated in these past studies. The effects of anions of the metal salts, however, have not been fully addressed. A recent study by Hunter et al.[34] found that Al^{3+} nitrate and perchlorate salts caused distinct LC behaviors; whereas 5CB coordinates to the perchlorate salt of Al^{3+} and assumes a homeotropic orientation, the LC exhibits a planar orientation on surfaces decorated with Al^{3+} nitrate salts. These results hint that the choice of anion can have a pronounced effect on the chemoresponsive properties of LC materials and motivated the study reported in this paper to understand more

[a] Department of Chemical and Biological Engineering, University of Wisconsin-Madison, 1415 Engineering Drive, Madison, Wisconsin 53706-1607, USA.
Email: emavrikakis@wisc.edu
Email: nlabbott@wisc.edu
[b] Department of Chemistry and Biochemistry, Kent State University, 1175 Risman Drive, Kent, Ohio 44242, USA.
† Authors contributed equally to this work.
Electronic Supplementary Information (ESI) available: See DOI: 10.1039/x0xx00000x

fully the role of anions on LC anchoring and to determine if the choice of anion can be exploited to optimize the response of LCs to targeted analytes.

Our approach to the elucidation of the role of anions is guided by recent advances in the use of computational chemistry to design and predict chemoresponsive LC systems.[35-37] In particular, Szilvási et al.[36] reported the first successful design of a chemoresponsive LC system based on first-principles calculations. Using two computational models, the Neutral Anion Model (NAM) and the Coordinatively Saturated Anion Model (CSAM), to calculate binding and displacement energies, they demonstrated that it is possible to predict the preferred orientation of LCs on metal salt-decorated surfaces, and whether or not specific analytes will trigger ordering transitions.[36,37] In this work, we build from these computational models to understand the effects of the anions in metal salts on chemoresponsive LC systems and thereby provide guidance to future designs of optimized chemoresponsive LC systems.

Our study here yields four key findings. First, in contrast to earlier findings based only on Al^{3+},[34] the NAM predictions and subsequent experimentation reveal that nitrate salts of other transition metal cations do bind nitrile-containing mesogens with sufficient strength to cause homeotropic LC orientations, a useful attribute for the design of chemoresponsive LC systems. Second, and also guided by computational predictions, we find that the coordination interactions of 5CB with surfaces presenting $La(NO_3)_3$, $Zn(NO_3)_2$, and $Co(NO_3)_2$ can be disrupted by DMMP, thus providing the first examples of chemoresponsive LCs based on metal-nitrate salts. Significantly, the observed response times with metal-nitrate salts are *faster* than those of the corresponding metal-perchlorate salts. Third, we find the orientations of the LC to be correlated across all metal cations investigated by a molecular anchoring energy density that is calculated as the product of the single-site binding energy and metal cation binding site density on the surface. Fourth, after incorporating the effects of water-mediated interactions into the free energy change associated with displacement of 5CB by DMMP from the metal cation binding site, we find that a universal exponential relationship exists between the calculated Displacement free energies (G_{DE}) and experimentally measured response times for both perchlorate and nitrate salts.

Methods

Theoretical

All calculations were performed using Gaussian 09.[38] The computational methodology, based on Density Functional Theory (DFT), is described in detail in our previous studies.[36,37] Geometry optimizations were carried out at the PW91/def2-SVP level of theory.[39,40] For more accurate energies, single point energy calculations were performed using the optimized geometries at the M06-2X-D3/def2-TZVP level of theory.[41,42] Thermodynamic correction terms were evaluated at 1 atm pressure and 298 K temperature at the PW91/def2-SVP level of theory. The thermodynamic corrections were then added to the higher level single point energies, affording free energies that are reported in this work.

The NAM and CSAM computational models are described in detail elsewhere[36,37] for metal-perchlorate salts. In the Supporting Information (SI), we briefly discuss the main features of these models for salts containing nitrate anions (Fig. S1). The compositions of the cluster model used in the NAM are consistent with the stoichiometric composition of metal salt used in the experiments. Therefore, this model describes the correct *global* composition of the metal salt. In the CSAM model, we use the same metal cation as in the NAM but we add perchlorates to fill the coordination shell of the metal cation, thus describing the *local* structure around the metal cations consistent with crystallographic measurements of perchlorate salts. Previously, we did not find a large difference between the predictive capability of the NAM and CSAM[37], but in the work presented in this paper, we find NAM to be superior to CSAM. Accordingly, we present and analyze the NAM results in the main body of this paper, while CSAM results are presented in the SI.

Binding free energies (G_{BE}) of molecules serving as surrogates of mesogens are calculated as $G_{BE} = G_{Model+LC} - G_{Model} - G_{LC}$, where $G_{Model+LC}$ is the total free energy of the metal salt cluster with the bound mesogen-surrogate, G_{Model} is the free energy of the naked metal salt cluster and G_{LC} is the free energy of the mesogen-surrogate molecule in the gas phase (Fig. S1). In our previous papers,[35,36] we determined that PhCN (Fig. S1) is a smaller but still useful surrogate molecule for 5CB. Negative values of G_{BE} (i.e., binding) were found to correlate with homeotropic ordering of 5CB whereas positive G_{BE} indicated planar ordering. Displacement free energies (G_{DE}) are calculated as the difference in G_{BE} of the mesogen (LC)-surrogate and that of the DMMP (Fig. S1, $G_{DE} = G_{BE\text{-}DMMP} - G_{BE\text{-}LC}$). If G_{DE} is more negative than a specified model-dependent threshold,[36,37] then we predict a LC response to arise from the favorable displacement reaction.

Experimental

Materials. Nickel(II) nitrate hexahydrate, Nickel(II) perchlorate hexahydrate, zinc(II) nitrate hexahydrate, zinc(II) perchlorate hexahydrate, lanthanum(III) nitrate hexahydrate, cobalt(II) nitrate hexahydrate, cobalt(II) perchlorate hexahydrate, iron(III) nitrate nonahydrate, iron(III) perchlorate hydrate, gallium(III) perchlorate nonahydrate, aluminum(III) nitrate nonahydrate, aluminum(III) perchlorate nonahydrate salts were purchased from Sigma-Aldrich (Milwaukee, WI). Gallium(III) nitrate nonahydrate and lanthanum(III) perchlorate hexahydrate were purchased from Alfa Aesar (Ward Hill, MA). Methanol and Fischer's Finest glass slides were purchased from Fischer Scientific (Pittsburgh, PA). Absolute ethanol (anhydrous, 200 proof) was purchased from Pharmco-AAPER (Brookfield, CT). All chemicals and solvents were of analytical reagent grade and were used as received without any further purification. All deionized water used in the study possessed a resistivity of at least 18.2 MΩ cm.

Formation of thin films of LC supported on metal salt-decorated surfaces. Glass slides were rinsed with copious amounts of ethanol and then dried under a stream of nitrogen. Metal ions were deposited onto the glass surfaces by spin coating ethanolic solutions of metal salts at the specified molar concentration (0.1-10 mM) at 3000 rpm for 30s (WS-400A-6NPP/Lite, Laurell Technologies, North Wales, PA). After coating the surface with metal salt, an 18 μm-thick copper TEM grid (Electron Microscopy Sciences, Hatfield, PA) was fastened to the surface by a thin stainless steel plate (0.44 mm thickness). The stainless steel plate contained a hole (diameter of 2mm) that was aligned with the TEM grid. The TEM grid was composed of squares with lateral dimensions of 285 μm and an overall diameter of 3 mm. Both the TEM grid and stainless steel plate were dip-coated with a perfluorocarbon (Nyebar Fluorocarbon Barrier Film, SmartGrease Company, Fairhaven, MA) layer to prevent wicking of the LC from the TEM grid. The grids were filled with LC using a microcapillary, taking care to fill the middle squares of the TEM grid only so as to avoid wicking of the LC away from the grid.

Exposure to DMMP. The LC-filled copper TEM grids were exposed to a stream of dry N_2 containing DMMP (10 ppm) within a flow cell with glass windows that permitted characterization of the optical appearance of the LC with a polarized optical microscope. A detailed description of the flow cell can be found in an earlier publication.[43] The flow system was plumbed using 1/16" stainless steel Swagelok tubing (Badger Fluid System Technologies, Milwaukee, WI). The gas containing DMMP was delivered to the flow cell at 100 ml/min by using a rotameter (Aalborg Instruments and Control, Orangeburg, NY). The optical appearance of the LC film was recorded using an Olympus camera (Olympus, Melville, NY) and WinTV software (Hauppauge, NY). The optical response of each LC film to DMMP was normalized by the maximum response (maximum intensity of transmitted light). The onset of exposure of the LC film to DMMP is denoted as t = 0 s in the plots reported in this paper. Error bars (standard deviations) are calculated from five repeat experiments unless stated otherwise.

Formation of LC films confined by two metal salt-decorated surfaces. Fiber spacers with 20 μm-diameters (EM Industries, Inc., Hawthorne, NY) were dispersed into Norland Optical Adhesive 65 (Norland Products, Inc., Cranbury, NJ). The perimeters of two metal salt-decorated glass surfaces were coated with the adhesive and the surfaces were adhered together by UV exposure for 30 minutes. A drop of 5CB, heated into its isotropic phase (T < 45°C), was then drawn by capillarity into the cavity between the two surfaces of the optical cell. The cell was subsequently cooled to room temperature.

Measurement of the birefringence of LC films. The birefringence of 5CB was measured using thin films confined between two metal salt-decorated surfaces. The retardance of each LC film was measured using a Berek compensator (Olympus, Melville, NY). The apparent birefringence of a LC sample was calculated from the retardance and thickness of the LC film, and the value of the tilt angle of the 5CB was determined from the known birefringence of 5CB.[22]

Measurement of the surface density of cation binding sites. After formation of metal salt-decorated glass surfaces, the metal salts were dissolved into 2% nitric acid. The concentration of metal salt was measured by using inductively coupled plasma optical emission spectrometry (ICP-OES, Perkin Elmer 4300). The surface density of the metal salt was calculated from both the ICP-OES data and knowledge of the area of the surface from which the metal salts were extracted. We note that this procedure yields an apparent density of cation binding sites available to the mesogens, as some cations may be buried within the salt layer on the surface and thus not accessible to mesogens. We used ellipsometry to determine that the optical thickness of a film of aluminum(III) perchlorate deposited from a 1mM ethanolic solution to be 1.6±0.3 nm, a thickness that corresponds to a few monolayers of the salt.

Results and discussion

Effect of anions on the anchoring behaviour of 5CB

Table 1 presents the free energy change upon binding (G_{BE}) of PhCN (surrogate for 5CB) to 14 unique metal salts (a combination of seven metal cations and two anions), as computed using the NAM. Inspection of Table 1 reveals that, as a consequence of strong binding, the NAM predicts homeotropic ordering of nematic 5CB on surfaces decorated with all the metal salts except for $Al(NO_3)_3$ (G_{BE} = 0.08 eV) and $Ga(NO_3)_3$ (G_{BE} = -0.03 eV). Table 1 also shows some general trends across metal cations and anions that have been evaluated in experiments as described subsequently. For example, the G_{BE} of any perchlorate salt is found to be more negative (indicating stronger binding) than that of the corresponding nitrate salt with the same metal cation.

Examination of the charge density difference plots (Fig. 1) of perchlorate and nitrate salts of Al^{3+} binding with PhCN provide insight into the results in Table 1. The plots show regions where the charge density of the bound complex increased or decreased relative to the free PhCN and the respective metal-anion complex. Fig. 1 indicates that there are subtle differences in charge accumulation and depletion regions for the perchlorate cluster as compared to the nitrate cluster. The lower charge accumulation with the nitrates can be traced to more negatively charged oxygen atoms in nitrates that donate more charge density to the metal cation. The nitrate anion has only three oxygens while the perchlorate anion has four oxygens over which to distribute the net negative charge of the anion. Mulliken charge analysis shows that the charge of an oxygen atom in a free nitrate anion is -0.50e while in a perchlorate anion it is only -0.42e (this difference in negative charge is compensated by the partial charge of the nitrogen and chlorine atoms to give both anions a net charge of -1). Similarly, the charge of the Al^{3+} center in the Al-perchlorate model is +0.82e whereas in the Al-nitrate model structure it is only +0.77e. These considerations underlie the result shown in Table 1 that PhCN binding is stronger with perchlorate as compared to nitrate anions.

Table 1 Calculated G_{BE} of PhCN to metal nitrate and metal perchlorate salts. All energy values are in eV.

	ClO_4^-	NO_3^-
Ni^{2+}	-1.04	-0.77
Zn^{2+}	-0.84	-0.65
La^{3+}	-0.84	-0.62
Co^{2+}	-0.76	-0.47
Fe^{3+}	-0.43	-0.33
Ga^{3+}	-0.54	-0.03
Al^{3+}	-0.40	+0.08

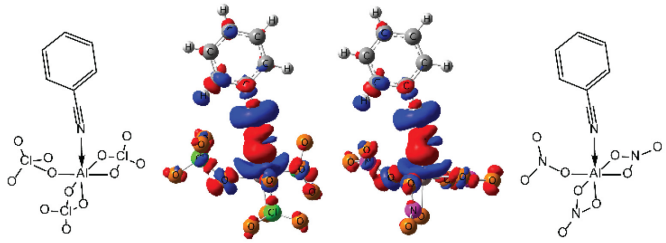

Fig. 1 Charge density difference plots for PhCN (surrogate of 5CB) bound to $Al(ClO_4)_3$ (left) and $Al(NO_3)_3$ (right). The corresponding schematic structures are shown on the far left and right, respectively. Blue and red, respectively, indicate the regions for charge depletion and charge accumulation.

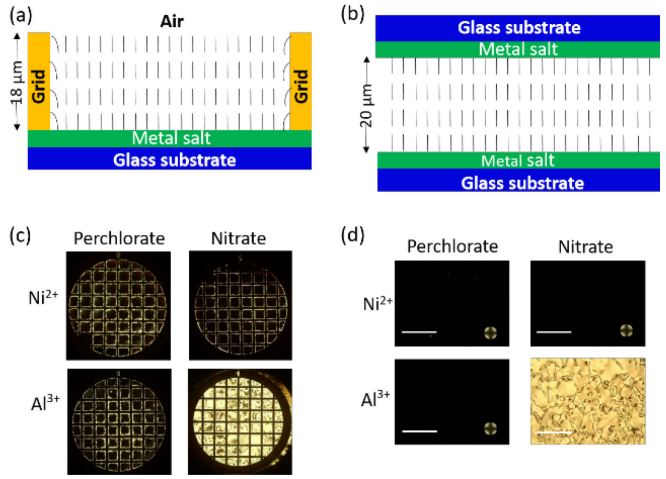

Fig. 2 Schematic illustration of the experimental setup and director profile of 5CB when (a) it is confined between a metal salt-decorated surface and an air interface or (b) when sandwiched between two metal salt-decorated glass interfaces. (c) Cross-polarized images of 5CB in the experimental setup shown in (a). (d) Cross-polarized images of 5CB confined between glass surfaces decorated with metal salts. In both (c) and (d), results are shown for Ni^{2+} and Al^{3+} salts. The scale bars represent 50 μm.

To test the predictions shown in Table 1, the anchoring of nematic 5CB on metal nitrate salt-decorated glass surfaces was investigated using either a copper TEM grid (Fig. 2a) or a sandwich cell (Fig. 2b). We used the two experimental set-ups because the LC hosted within a TEM grid has an air-LC interface that is homeotropic (Fig. 2a), which can influence conclusions regarding the orientation of the LC film at the solid-LC interface. In contrast, the sandwich cell has two salt-coated LC surfaces (Fig. 2b). In the sandwich cell geometry, homeotropic anchoring at the metal salt-coated surface is evidenced by the absence of transmitted light under crossed polarizers and degenerate planar/tilted anchoring is characterized by Schlieren-like textures. Representative images of nematic 5CB supported on surfaces decorated with metal (Ni^{2+} or Al^{3+}) perchlorate and nitrate salts are shown in Fig. 2c and 2d (others can be found in SI, Fig. S2). Our measurements with the sandwich cells revealed homeotropic anchoring of 5CB for $Ni(NO_3)_2$, $Zn(NO_3)_2$, $La(NO_3)_3$, $Co(NO_3)_2$, and $Fe(NO_3)_3$ whereas $Ga(NO_3)_3$ and $Al(NO_3)_3$ caused tilted or planar anchoring of 5CB.

Before comparing the experimental results with the theoretical predictions, we explored the possibility that the tilted/planar anchoring observed in experiments with Ga^{3+} and Al^{3+} nitrate salts was a consequence of insufficient surface density of the metal cation binding sites on the surfaces. It has been shown previously that planar anchoring is observed at sufficiently low metal cation binding site densities even when individual sites bind strongly to 5CB.[36] We deposited the metal salts from ethanolic solutions containing 10 mM of the salt and measured the surface densities of metal perchlorate and nitrate salts coated on glass surfaces using ICP-OES. Our measurements revealed that the surface densities of all fourteen metal salts in Table 1 are remarkably similar (99 ± 2 pmol/mm^2). Additional details are provided in SI (Fig. S3). This result demonstrates that the anchoring behaviors of 5CB on the surfaces decorated with nitrate salts of Ga^{3+} and Al^{3+} do reflect the different binding strengths of the metal salts with 5CB. We quantified the tilt angle of 5CB (away from the normal) by performing measurements of the optical retardance of the LC films (see Methods). The tilt angle of the nematic film of 5CB at the surfaces decorated with nitrate salts of Ga^{3+} and Al^{3+} were measured to be almost 90º from the surface normal, as shown in Fig. S4 (within uncertainty in the measurement). This measurement indicates that the anchoring of the LC is planar on these two surfaces. In contrast, we note that perchlorate salts of these two metals cause homeotropic anchoring of the LC.

Fig. 3 presents a comparison of the calculated values of G_{BE} to the experimentally observed anchoring behavior. Inspection of Fig. 3 reveals agreement between the experiments and the theoretical predictions for thirteen of fourteen of the salts. Disagreement is observed formally for $Ga(NO_3)_3$, for which G_{BE} was calculated to be -0.03 eV, a value that is very close to the threshold 0 eV. We note, however, that this apparent disagreement is not statistically significant because the uncertainty of typical DFT calculations can be as large as 0.10-0.20 eV.[44]

To evaluate further the theoretical predictions of the binding energies of 5CB to the metal binding sites of metal salt-coated surfaces, we performed a series of experiments in which we prepared surfaces with decreasing surface densities of metal cation binding sites. Specifically, we sought to determine the lowest surface density (LSD) of metal cation binding sites for which homeotropic anchoring of the LC was observed. For this experiment, we selected three metal salts, $Ni(ClO_4)_2$, $Zn(ClO_4)_2$, and $Ga(ClO_4)_3$. Our experimental results (Fig. 4a) reveal that the LSDs for these three metal perchlorate salts are 3.3 pmol/mm^2, 4.3 pmol/mm^2, and 6.2 pmol/mm^2, respectively. The measured order of the LSDs is consistent (via an inverse relationship) with the predicted G_{BE} ($Ni(ClO_4)_2$: -1.04 eV, $Zn(ClO_4)_2$: -0.84 eV, and $Ga(ClO_4)_3$: -0.54 eV).

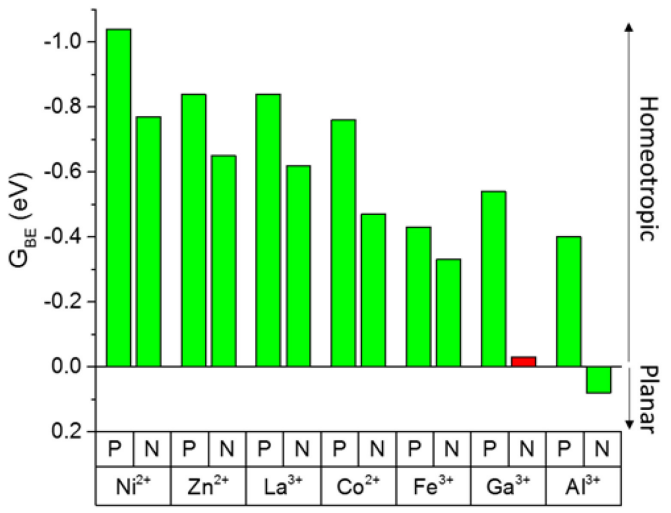

Fig. 3 Comparison of experimentally observed orientations of 5CB on various metal salt-decorated surfaces and calculated values of G_{BE} of PhCN. Homeotropic anchoring is predicted to occur when G_{BE} is negative. "N" and "P" on the x axis refer to nitrate and perchlorate anions, respectively. Green bars represent agreement between theoretical predictions and experimental observations, whereas the red bar shows disagreement.

A second general prediction of the theory is that binding of PhCN is stronger for perchlorates as compared to the corresponding nitrate salts (Table 1). We tested this prediction by determining the LSDs of nitrate and perchlorate salts of Ni^{2+}. Inspection of Fig. 4b reveals that the LSD is larger for $Ni(NO_3)_2$ (4.6 pmol/mm^2) than $Ni(ClO_4)_2$ (3.2 pmol/mm^2), consistent with the stronger binding of 5CB to the perchlorate salt (-1.04 eV) than nitrate salt (-0.77 eV).

We used the LSD measurements and G_{BE} calculations, as described above, to determine if one can predict the orientational behavior of the LC using a calculated "molecular surface anchoring energy density". Motivated by our proposal that homeotropic anchoring can be induced by a small number of very strongly bound mesogens or, conversely, a large number of weakly bound mesogens on the surface, we calculated a surface anchoring energy as the product of the LSD and G_{BE} for each salt. Consistent with this model, Fig. 4c reveals that the LSD and G_{BE} are inversely related (R^2 = 0.98). The constant of the relationship is -3.5 pmol·eV/mm^2 = -0.34 J/m^2 which is an estimate of the molecular anchoring energy per area required to induce homeotropic anchoring for 5CB. Past molecular dynamics simulations have reached similar conclusions regarding the order of magnitude of molecular anchoring energies at crystalline (cristobalite) and amorphous (silica) surfaces.[45,46] We note that experimental measurements of anchoring energies are typically orders of magnitude smaller than molecular anchoring energies, which reflects the fact that experiments typically measure the reorientation of micrometer-thick films of LC that occur with only minor perturbation to the orientation of the mesogens adsorbed at the confining surface.

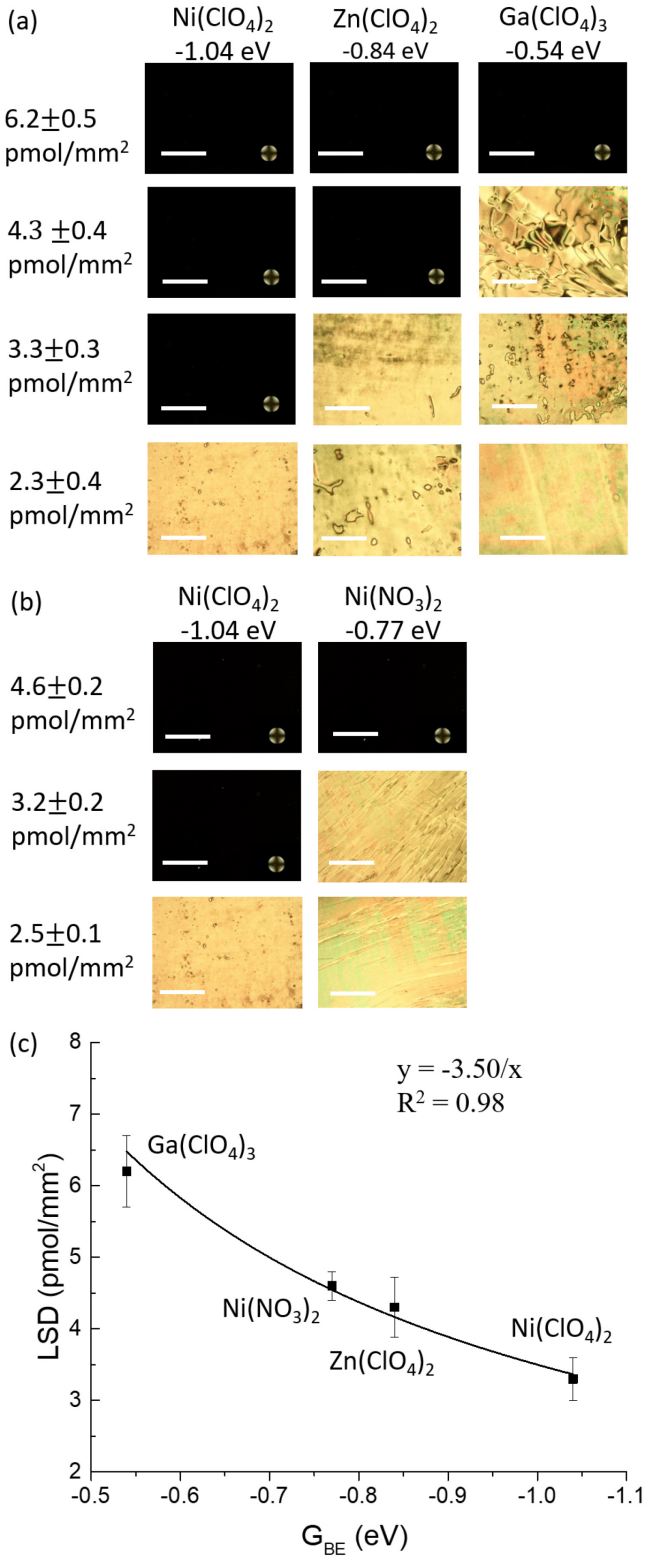

Fig. 4 (a) Cross-polarized images of 5CB films in contact with surfaces coated with $Ni(ClO_4)_2$, $Zn(ClO_4)_2$, and $Ga(ClO_4)_3$. The values of surface density are shown in the left column. (b) Anchoring behaviours of nickel perchlorate and nitrate salts with different surface densities. (c) Plot of the measured LSD from (a) and (b) versus calculated G_{BE}. The scale bars represent 50 μm.

Effect of anions on adsorbate-driven change in anchoring of 5CB

Next we calculated the change in free energy accompanying displacement of 5CB by DMMP from a metal salt complex (G_{DE}). Calculations predict negative values of G_{DE} (Table 2). Our past experience revealed[36,37] that a threshold value of -0.50 eV correlated with the onset of experimentally observed displacement processes, as governed by the kinetics of the response (see details in the Methods section and in the SI as well). Using this threshold value, we predicted that the following metal salts would trigger a response in 5CB upon exposure to DMMP: $Zn(ClO_4)_2$, $La(ClO_4)_3$, $Co(ClO_4)_2$, $Fe(ClO_4)_3$, $Ga(ClO_4)_3$, $Al(ClO_4)_3$, $La(NO_3)_3$, and $Co(NO_3)_2$. Inspection of Table 2 also reveals the general trend that the magnitude of G_{DE} for nitrate salts was generally similar to or smaller in magnitude than the corresponding perchlorate salt, suggesting that the rate of response of the LC with some nitrate salts will be slower than perchlorate salts.

Fig. 5a shows a representative example of the optical response (between crossed polarizers) of nematic 5CB on surfaces decorated with $Co(NO_3)_2$ (density 99 ± 2 pmol/mm^2) before and after exposure to DMMP. Prior to exposure, each sample was equilibrated by exposure to dry N_2. A gaseous stream containing 10 ppm DMMP was subsequently introduced over the 5CB film. The competitive binding of DMMP and 5CB at the salt-coated surface disrupts the homeotropic anchoring of 5CB and leads to the transmission of polarized light through the LC sample. The change in optical appearance of the LC film was reversible upon reexposure of the sample to dry N_2. Our experiments demonstrated that $Ni(ClO_4)_2$, $Co(ClO_4)_2$, $Ni(NO_3)_2$, and $Fe(NO_3)_3$ did not show a response while $Zn(ClO_4)_2$, $La(ClO_4)_3$, $Fe(ClO_4)_3$, $Ga(ClO_4)_3$, $Al(ClO_4)_3$, $Zn(NO_3)_2$, $La(NO_3)_3$, and $Co(NO_3)_2$ all showed a response.

Fig. 5b compares the theoretical predictions to our experimental measurements of the response of 5CB upon exposure to DMMP. Overall, inspection of Fig. 5b reveals good qualitative agreement between experiments and model calculations; ten of eleven cases are found to be in agreement. The single outlier is $Co(ClO_4)_2$. This discrepancy might be explained by the open d-shell of Co^{2+} that is more difficult to model than closed shell species.[36]

Table 2. Calculated G_{DE} of PhCN by DMMP. All energy values are in eV. $Al(NO_3)_3$ and $Ga(NO_3)_3$ results are omitted because of the lack of homeotropic ordering of 5CB in these systems.

	ClO_4^-	NO_3^-
Ni^{2+}	-0.47	-0.41
Zn^{2+}	-0.57	-0.50
La^{3+}	-0.64	-0.57
Co^{2+}	-0.66	-0.66
Fe^{3+}	-0.66	-0.40
Ga^{3+}	-0.66	-
Al^{3+}	-0.74	-

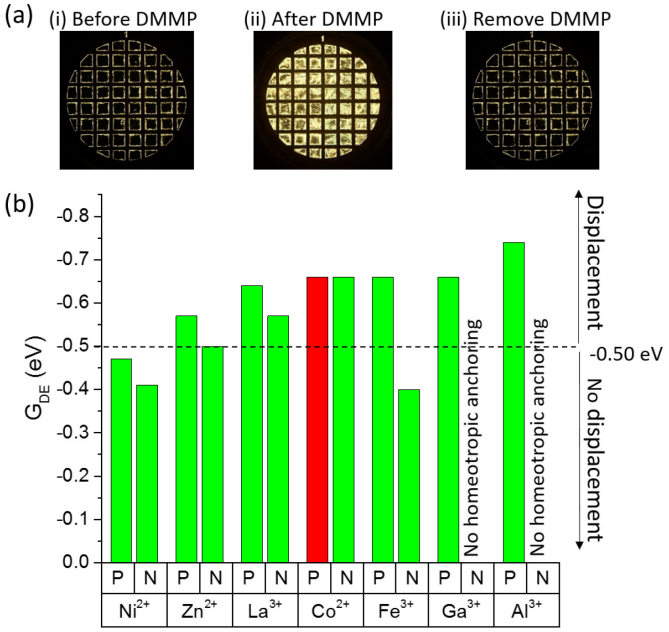

Fig. 5 (a) Cross-polarized images of 5CB in experiments performed with $Co(NO_3)_2$ on glass surfaces (i) before exposure to 10 ppm DMMP (ii) after exposure to 10 ppm DMMP for 30 minutes (iii) sample exposed to DMMP is further exposed to dry N2 for 30 minutes. (b) Comparison of experimental response to DMMP and calculated G_{DE} of PhCN. Displacement is predicted to occur when the displacement free energy is -0.50 eV or more negative. "N" and "P" on the x axis refer to nitrate and perchlorate anions, respectively. Green bars represent agreement between theoretical predictions and experimental observations, whereas red bars show disagreement.

An important result in Fig. 5b is the observation that three metal nitrate salts, $Zn(NO_3)_2$, $La(NO_3)_3$ and $Co(NO_3)_2$, exhibit orientational transitions and thus optical responses upon exposure to DMMP. We emphasize that the results reported in this paper are the first experimental observation of a chemoresponsive LC designed using metal nitrate salts. The only prior report has involved the use of $Al(NO_3)_3$, wherein it was correctly reported that 5CB supported on $Al(NO_3)_3$ salts does not respond to DMMP.[34]

We performed additional characterization of the chemoresponsive properties of the LCs on the perchlorate and nitrate salts by quantifying the dynamics of the response of the LCs to DMMP. We define as *characteristic response time* the interval of time between the introduction of the analyte and measurement of 80% of the normalized light intensity of the full response (see details in the Methods Section). Fig. 6a shows that the characteristic response times for the perchlorate salts (black dots) varied in a roughly exponential manner with G_{DE} (R^2 = 0.58), similar to previous reports in the literature.[35,36]

However, further inspection of Fig. 6a reveals that nitrate salts do not conform to the exponential function displayed by the perchlorates. Specifically, the responses of $La(NO_3)_3$ and $Zn(NO_3)_2$ are found far from the perchlorates curve. The qualitative disagreement between the experimental response times and G_{DE} prompted us to explore if there is an experimental feature that needs to be incorporated in the model to find a universal relationship that covers both nitrate and perchlorate salts.

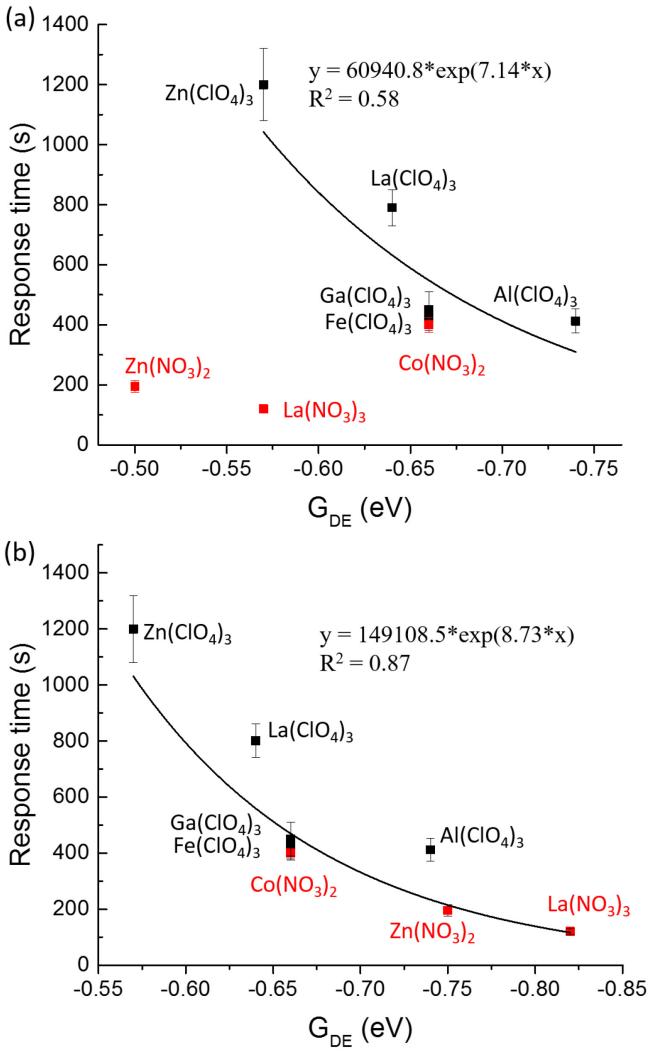

Fig. 6 Experimental response time of 5CB anchored to various metal salts upon exposure to DMMP as a function of the calculated G_{DE}. (a) Exponential curve fitted using only perchlorate salt results. (b) Exponential curve fitted using all metal salt results after water correction.

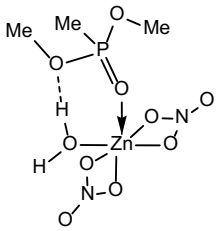

Fig. 7 Schematic representation of hydrogen bonding between the methoxy groups of DMMP and a water molecule present in the coordination shell of Zn^{2+} for the $Zn(NO_3)_2$ model structure. Dashed line indicates the hydrogen bond. Arrow refers to the binding of DMMP to the metal center.

We hypothesized, in particular, that water associated with the metal cation binding sites may be important. This direction of inquiry was based on the observation that $Zn(NO_3)_2$ and $La(NO_3)_3$ do not cause homeotropic anchoring of 5CB at elevated relative humidity (> 28%; see details in SI). We postulate that the change in the local environment of the metal cations as determined by the presence of water molecules could influence the measured response times. Specifically, water molecules in the metal coordination sphere can also hydrogen bond with DMMP at the same site (Fig. 7). DMMP contains unbound oxygen atoms that can form hydrogen bonds with water molecules in the coordination shell of the metal cation. This hydrogen bonding can formally increase the binding of DMMP to the surface thus shifting the respective value of G_{DE} to the right in Fig. 6. It is important to note that there are no oxygens or any other available functional groups in 5CB that can also form hydrogen bonds to increase the binding of 5CB to the metal site. We calculated the binding strength of a water molecule with the methoxy oxygen of DMMP (-0.25 eV) and accordingly corrected the G_{DE} for $Zn(NO_3)_2$ and $La(NO_3)_3$ by -0.25 eV as they showed extreme sensitivity to relative humidity. In contrast to the nitrate salts, we do not observe perchlorate salts of metal cations to show comparable levels of sensitivity to humidity.

Fig. 6b shows the experimental response times plotted against the G_{DE} values corrected for hydrogen bonding. After applying this correction, all the data points fall on a monotonic exponential curve between response times and G_{DE}. Specifically, the data obtained using nitrate and perchlorate salts fall onto a universal curve (R^2 = 0.87). These results show that a universal exponential relationship can be found for all metal salt surfaces, independent of the choice of anion or cation. We anticipate this conclusion will also be valid for mesogens other than 5CB, demonstrating a universal behavior of LCs anchored on surfaces presented well-defined binding sites.

The computational results presented in this paper were evaluated using the NAM to describe binding of mesogens to metal cation sites. Previously, we evaluated two different models (NAM and CSAM) for these binding events and concluded that NAM is preferred for prediction of binding of mesogens to metal cations whereas CSAM is preferred for describing the displacement of the mesogens by the analyte.[37] As detailed in Supporting Information, we explored the use of CSAM for nitrate ions, and found that it did not accurately predict nitrile groups to bind to the cations of $Ni(NO_3)_2$, $Zn(NO_3)_2$, and $Co(NO_3)_2$ (Table S1). Therefore, we conclude that the NAM represents a more accurate model of the interactions reported in this paper.

Conclusions

Using computational chemistry guidance, we show that the anion of transition metal salts can have a profound influence on the chemoresponsive properties of LCs ordered on transition metal salt-decorated surfaces. Although both experiment and computation support the conclusion that the binding of nitrile groups to metal cation centers is weakened when using nitrate salts (as compared to perchlorate salts), we have found that $La(NO_3)_3$, $Zn(NO_3)_2$, and $Co(NO_3)_2$ provide the basis of chemoresponsive LCs that have dynamic properties that are superior to perchlorate-based chemoresponsive LCs. Specifically, when using nitrate salts, the observed response to DMMP is 6 times *faster* than that of the corresponding metal perchlorate salts. This observation is explained by participation

of water in the metal nitrate binding complex, with favorable hydrogen bonding between water and DMMP, but not 5CB. By incorporating the role of water in the calculation of the displacement free energy, we find an exponential relationship between the displacement free energy and response rate that spans all perchlorate and nitrate salts. In addition, we find the orientations of the LC to be correlated across all metal cations investigated by a molecular anchoring energy density that is calculated as the product of the single-site binding energy and metal cation binding site density on the surface. This characteristic of surfaces decorated with metal binding sites for mesogens distinguishes our approach from the majority of past studies of the anchoring of LCs on polymeric surfaces, at which van der Waals interactions, which are difficult to manipulate in a predictable manner, dominate the orientational ordering of LCs. Overall, surfaces decorated with metal binding sites for LCs appear a versatile class of surfaces for future fundamental studies of the surface anchoring of LCs.

Conflicts of interest

N. L. A. declares a financial interest in Platypus Technologies LLC, a for-profit company that has developed LC-based analytic technologies.

Acknowledgements

This work was supported by the National Science Foundation (DMREF grant DMR-1435195) and the Army Research Office (W911NF-14-1-0140). Calculations were performed at supercomputing centers located at the Environmental Molecular Sciences Laboratory (EMSL), which is sponsored by the Department of Energy (DOE) Office of Biological and Environmental Research at Pacific Northwest National Laboratory (PNNL); the Center for Nanoscale Materials (CNM) at Argonne National Laboratory (ANL), supported by DOE Contract DE-AC02-06CH11357; and the National Energy Research Scientific Computing Center (NERSC), supported by DOE Contract DE-AC02-05CH11231. Facilities of the Wisconsin MRSEC were used in this work (DMR-1121288).

Notes and references

1 R. R. Shah and N. L. Abbott, *Science*, 2001, **293**, 1296−1299.
2 R. R. Shah and N. L. Abbott, *Langmuir*, 2003, **19**, 275−284.
3 B. Jerome, *Rep. Prog. Phys.,* 1991, **54**, 391−451.
4 H. Yokoyama, *Mol. Cryst. Liq. Cryst*., 1988, **165**, 265−316.
5 P. N. Sanda, D. B. Dove, H. L. Ong, S. A. Jansen and R. Hoffmann, *Phys. Rev. A*, 1989, **39**, 2653−2658.
6 V. G. Nazarenko and O. D. Lavrentovich, *Phys. Rev. E*, 1994, *49*, R990-R993.
7 S. H. Perlmutter, D. Doroski and G. Moddel, *Appl. Phys. Lett.*, 1996, **69**, 1182-1184.
8 V. G. Nazarenko, V. M. Pergamenshchik, O. V. Koval'chuk, A. B. Nych and B. I. Lev, *Phys. Rev. E*, 1999, **60**, 5580–5583.
9 R. R. Shah and N. L. Abbott, *J. Phys. Chem. B*, 2001, **105**, 4936-4950.
10 G. Barbero and D. Olivero, *Phys. Rev. E*, 2002, **65**, 031701.
11 H. A. Pereira, F. Batalioto and L. R. Evangelista, *Phys. Rev. E*, 2003, **68**, 040701.
12 H. A. Pereira, F. Batalioto and L. R. Evangelista, *Eur. Phys. J. E*, 2005, **16**, 267-272.
13 L. R. Evangelista, G. Barbero, *Liquid Cryst*. 2006, **33**, 1–15.
14 J. T. Hunter, S. K. Pal and N. L Abbott, *ACS Appl. Mater. Interfaces*, 2010, **2**, 1857−1865.
15 K. L. Yang, K. Cadwell and N. L. Abbott, *J. Phys. Chem. B*, 2004, **108**, 20180−20186.
16 J. T. Hunter and N. L Abbott, *Sens. Actuators B*, 2013, **183**, 71−80.
17 A. Abu-Abed, R. G. Lindquist and W.-H. Choi, *IEEE Sens. J.,* 2007, **7**, 1617-1624
18 W. F. Ho, H. P. Chan and K. L Yang, *IEEE Sens. J.,* 2013, **13**, 2521-2522.
19 P. Cachelin J. P. Green, T. Peijs, M. Heeney and C. W. M. Bastiaansen, *Adv. Optical Mater*., 2016, **4**, 592–596.
20 J. M. Brake, M. K. Daschner, Y.-Y. Luk and N. L. Abbott, *Science*, 2003, **302**, 2094-2097.
21 V. J. Aliño, P. H. Sim, W. T. Choy, A. Fraser and K.-Y. Yang, *Langmuir,* 2012, **28**, 17571–17577.
22 N. A. Lockwood, J. K. Gupta and N. L Abbott, *Surf. Sci. Rep*., 2008, **63**, 255-293.
23 R. J. Carlton, J. T. Hunter, D. S. Miller, R. Abbasi, P. C. Mushenheim, L. N. Tan and N. L. Abbott, *Liq. Cryst. Rev.,* 2013, **1**, 29-51.
24 X. Su, S. Voskian, R. P. Hughes and I. Aprahamian, *Angew. Chem. Int. Ed*., 2013, **52**, 10734-10739.
25 S. S. Sridharamurthy, K. D. Cadwell, N. L. Abbott and H. Jiang, *Smart Mater. Struct*. 2008, **17**, 012001.
26 K. D. Cadwell, M. E. Alf and N. L. Abbott, *J. Phys. Chem. B*, 2006, **110**, 26081−26088.
27 K. D. Cadwell, N. A. Lockwood, B. A. Nellis, M. E. Alf, C. R. Willis and N. L. Abbott, *Sens. Actuators B*, 2007, **128**, 91−98.
28 D. M. Cheng, S. S. Sridharamurthy, J. T. Hunter, J. Park, N. L. Abbott and H. Jiang, *J. Microelectromech. Syst.,* 2009, **18**, 973−982.
29 J. T. Hunter and N. L. Abbott, In Liquid Crystals Beyond Displays: Chemistry, Physics, and Applications; Li, Q., Ed.; Wiley: Hoboken, NJ, 2012; pp 485−505.
30 S. K. Pal, C. Acevedo-Velez, J. T. Hunter and N. L. Abbott, *Chem. Mater*., 2010, **22**, 5474−5482.
31 K. L. Yang, K. Cadwell and N. L. Abbott, *Sens. Actuators B*, 2005, **104**, 50−56
32 P.-H. Wang, J.-H. Yu, Y.-B. Zhao, Z.-J. Li and G.-Q. Li, *Sens. Actuators B,* 2011, **160**, 929−935.
33 H. J. VanTreeck, D. R. Most, B. A. Grinwald, K. A. Kupcho, A. Sen, M. D. Bonds and B. R. Acharya, *Sens. Actuators B*, 2011, **158**, 104−110.
34 J. T. Hunter and N. L. Abbott, *ACS Appl. Mater. Interfaces,* 2014, **6**, 2362-2369.
35 L. T. Roling, J. Scaranto, J. A. Herron, H. Yu, S. Choi, N. L. Abbott and M. Mavrikakis, *Nat. Commun.* 2016, **7**, 13338.
36 T. Szilvási, L. T. Roling, H. Yu, P. Rai, S. Choi, R. J. Twieg, M. Mavrikakis and N. L. Abbott, *Chem. Mater*., 2017, **29**, 3563−3571.
37 H. Yu, T. Szilvási, P. Rai, R. J. Twieg, M. Mavrikakis and N. L. Abbott, *submitted*.
38 M. J. Frisch, G. W. Trucks, H. B. Schlegel, G. E. Scuseria, M. A. Robb, J. R. Cheeseman, G. Scalmani, V. Barone, G. A. Petersson, H. Nakatsuji, X. Li, M. Caricato, A. V Marenich, J. Bloino, B. G. Janesko, R. Gomperts, B. Mennucci, H. P. Hratchian, J. V Ortiz, A. F. Izmaylov, J. L. Sonnenberg, D. Williams-Young, F. Ding, F. Lipparini, F. Egidi, J. Goings, B. Peng, A. Petrone, T. Henderson, D. Ranasinghe, V. G. Zakrzewski, J. Gao, N. Rega, G. Zheng, W. Liang, M. Hada, M. Ehara, K. Toyota, R. Fukuda, J. Hasegawa, M. Ishida, T. Nakajima, Y. Honda, O. Kitao, H. Nakai, T. Vreven, K. Throssell,

J. A. Montgomery Jr., J. E. Peralta, F. Ogliaro, M. J. Bearpark, J. J. Heyd, E. N. Brothers, K. N. Kudin, V. N. Staroverov, T. A. Keith, R. Kobayashi, J. Normand, K. Raghavachari, A. P. Rendell, J. C. Burant, S. S. Iyengar, J. Tomasi, M. Cossi, J. M. Millam, M. Klene, C. Adamo, R. Cammi, J. W. Ochterski, R. L. Martin, K. Morokuma, O. Farkas, J. B. Foresman, D. J. Fox, Gaussian 09 Revision D.01 2009.

39 J. P. Perdew and Y. Wang, *Phys. Rev. B,* 1992, **45**, 13244−13249.

40 F. Weigend and R. Ahlrichs, *Phys. Chem. Chem. Phys.,* 2005, **7**, 3297−3305.

41 Y. Zhao and D. G. Truhlar, *Theor. Chem. Acc.,* 2008, *120*, 215−241.

42 S. Grimme, J. Antony, S. Ehrlich, H. Krieg, *J. Chem. Phys.,* 2010, **132**, 154104.

43 J. T. Hunter and N. L. Abbott, *Sens. Actuators B,* 2013, **183**, 71−80.

44 K. E. Riley, B. T. Op't Holt and K. M. Merz, *J. Chem. Theory Comput.*, 2007, **3**, 407-433.

45 A. Pizzirusso, R. Berardi, L. Muccioli, M. Ricci and C. Zannoni, *Chem. Sci.*, 2012, **3**, 573−579.

46 O. M. Roscioni, L. Muccioli, R. G. Della Valle, A. Pizzirusso, M. Ricci, C. Zannoni, Langmuir, 2013, 29, 8950−8958.

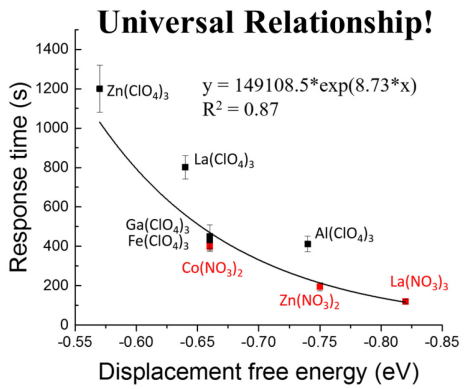

Universal exponential relationship is found between calculated displacement free energies and measured dynamic response of liquid crystals to adsorbates for all studied metal salts.

SUPPLEMENTARY MATERIAL

The Role of Anions in Adsorbate-induced Anchoring Transitions of Liquid Crystals on Surfaces with Discrete Cation Binding Sites

Tibor Szilvási[a,†], Nanqi Bao[a,†], Huaizhe Yu,[a] Robert J. Twieg[b], Manos Mavrikakis[a,*], Nicholas L. Abbott[a,*]

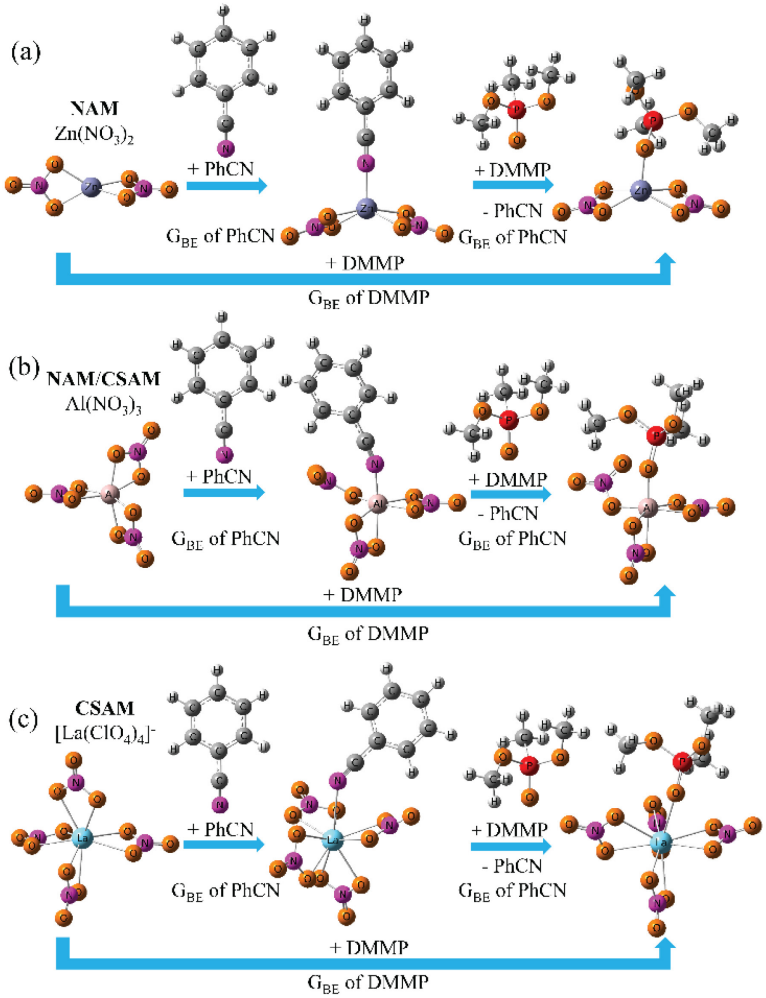

Figure S1. Representative structures from which G_{BE} and G_{DE} were calculated. (a) NAM structure for $Zn(NO_3)_2$ (left structure), its interaction with PhCN (middle structure), and DMMP (right structure). (b) CSAM and NAM structure for $Al(NO_3)_3$ (left structure), its interaction with PhCN (middle structure), and DMMP (right structure). (c) CSAM structure for $[La(NO_3)_4]^-$ (left structure), its interaction with PhCN (middle structure), and DMMP (right structure).

The NAM consists of a metal cation, in its most stable oxidation state, and anions are added to neutralize the cluster model. A model structure of $Zn(NO_3)_2$ and $Al(NO_3)_3$ is shown in Figure S1a and S1b, respectively. The NAM describes the right global composition of the metal salt while the metal cations are relatively under-coordinated. We previously hypothesized that this under-coordination can be present on metal salt surfaces thus NAM can be very useful to predict homeotropic ordering.

The CSAM model also contains a metal cation and anions are added to fill the coordination shell of the metal cation. Examples for CSAM, $Al(NO_3)_3$ and $[La(NO_3)_4]^-$, are shown in Figure S1b and S1c, respectively. We note that the definition of NAM and CSAM results in the same structure for Al^{3+}, Fe^{3+}, and Ga^{3+}. Also, the CSAM model structures can be negatively charged as shown in Figure S1c for $[La(NO_3)_4]^-$. CSAM provides somewhat over-coordinated metal cations which may be good candidates to describe the metal cation environment after homeotropic ordering thus predict response properties.

Table S1. Calculated G_{BE} of PhCN using NAM and CSAM. All energy values are in eV. Dashed lines indicate the lack of a stable bound structure.

Anion	ClO_4^-		NO_3^-	
Model	NAM	CSAM	NAM	CSAM
Ni^{2+}	-1.04	0.09	-0.77	---
Zn^{2+}	-0.84	0.03	-0.65	---
La^{3+}	-0.84	-0.20	-0.62	-0.07
Co^{2+}	-0.76	0.40	-0.47	---
Fe^{3+}	-0.43	-0.43	-0.33	-0.33
Ga^{3+}	-0.54	-0.54	-0.03	-0.03
Al^{3+}	-0.40	-0.40	0.08	0.08

Table S2. Calculated G_{DE} of PhCN using NAM and CSAM. All energy values are in eV. Dashed lines indicate the lack of a stable bound structure of PhCN and metal nitrate model cluster during energy minimization. 'x' signifies the lack of homeotropic ordering.

Anion	ClO_4^-		NO_3^-	
Model	NAM	CSAM	NAM	CSAM
Ni^{2+}	-0.47	-0.27	-0.41	---
Zn^{2+}	-0.57	-0.38	-0.50	---
La^{3+}	-0.64	-0.55	-0.57	-0.44
Co^{2+}	-0.66	-0.58	-0.66	---
Fe^{3+}	-0.66	-0.66	-0.40	-0.40
Ga^{3+}	-0.66	-0.66	x	x
Al^{3+}	-0.74	-0.74	x	x

Table S2 shows the calculated G_{DE} of DMMP for all studied metal salts. Dashed lines indicate the lack of G_{DE} of DMMP. This is because of the absence of a stable bound structure of PhCN for those metal salts (see Table S1). For the rest of the metal salts, the calculations predict negative G_{DE} values, but it is important to remember that because of the model-dependent threshold, (see Methods section) this does not necessarily mean that an experimental response would be observed.

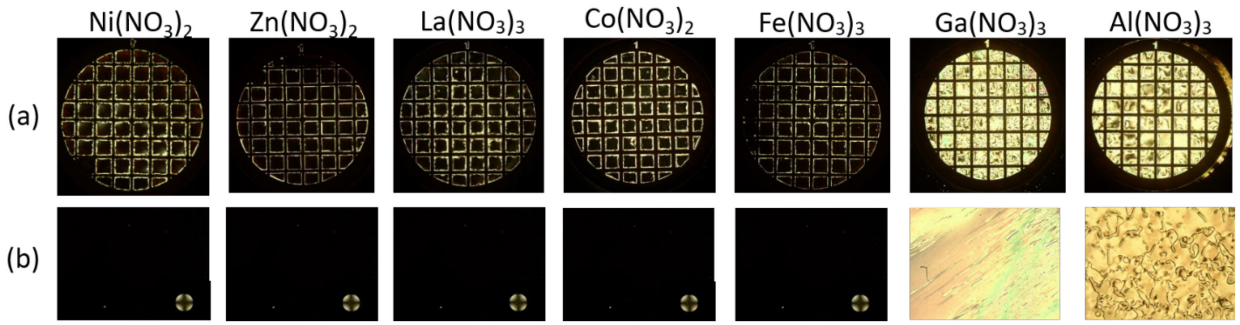

Figure S2. Cross-polarized images of 5CB films (a) in the experiment setup a and (b) in the experiment setup b in Figure 2 on the metal nitrate salts-decorated glasses.

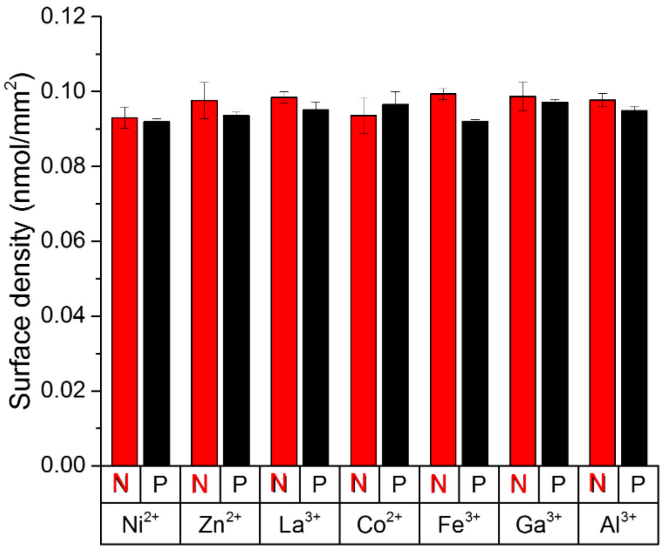

Figure S3. Surface density of metal salts coated on glass surface measured using ICP-OES. The concentration of metal salts is 10 mM in ethanolic solution. "N" and "P" on the x axis refer to nitrate and perchlorate anions, respectively.

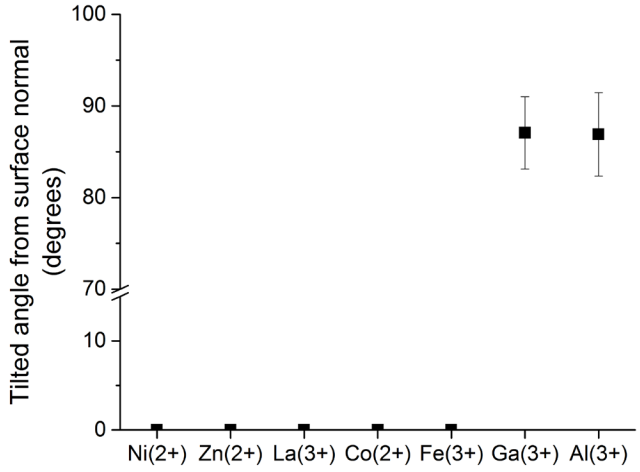

Figure S4. Tilt angle with respect to the surface normal for 5CB in experimental setup b in Figure 2 using retardance measurements.

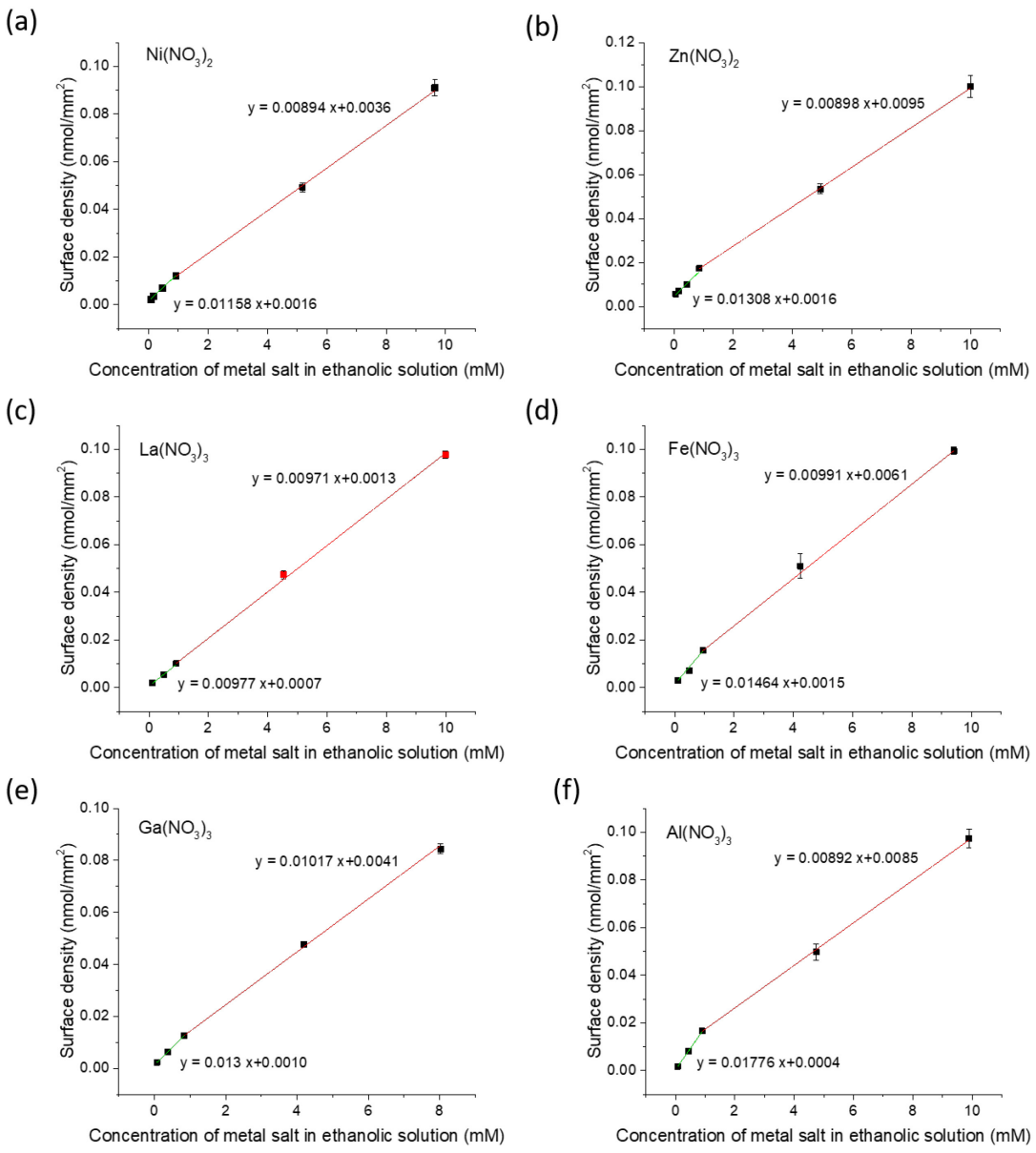

Figure S5. Surface density of metal nitrate salts coated on glass surface as a function of its concentration in ethanolic solution as coating solution. There are two fitting regions for each metal salt: one is from 1 mM to 10 mM (x axis); the other is from 0.1 mM to 1 mM. Metal salts: (a) $Ni(NO_3)_2$ (b) $Zn(NO_3)_2$ (c) $La(NO_3)_3$ (d) $Fe(NO_3)_3$ (e) $Ga(NO_3)_3$ (f) $Al(NO_3)_3$.

Two fitting regions (1 mM to 10 mM, and 0.1 mM to 1 mM) were decided based on fitting correlations. In these six plots, the slop of the region with lower concentration is always larger than that of the region with higher concentration. This could be due to different viscosities. The viscosity of coating solution is a key factor in spin-coating process: thicker coating can be obtained using solutions with higher viscosity under the same coating condition. So, if we suppose that the viscosity of coating solution in lower concentration region (0.1 mM to 1 mM) is constant and lower, the surface density should be smaller than what we get based on red linear fitting lines.

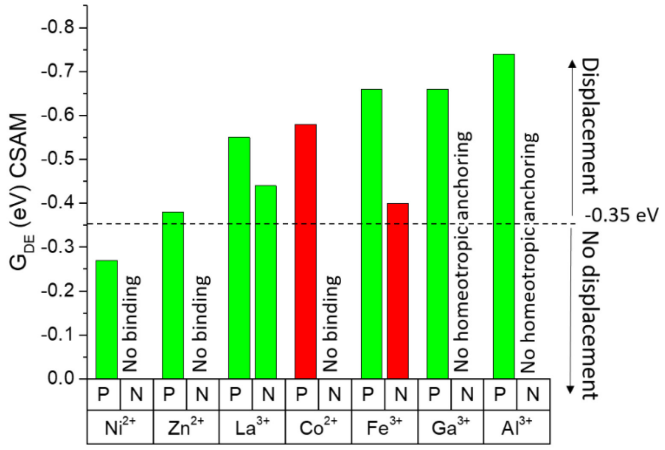

Figure S6. Comparison of experimental response to DMMP and calculated G_{DE} of PhCN using the CSAM. Displacement is predicted to occur when the displacement free energy is more negative than -0.35 eV. "N" and "P" on the x axis refer to nitrate and perchlorate anions, respectively. Green bars represent agreement between theoretical predictions and experimental observations, whereas red bars show disagreement.

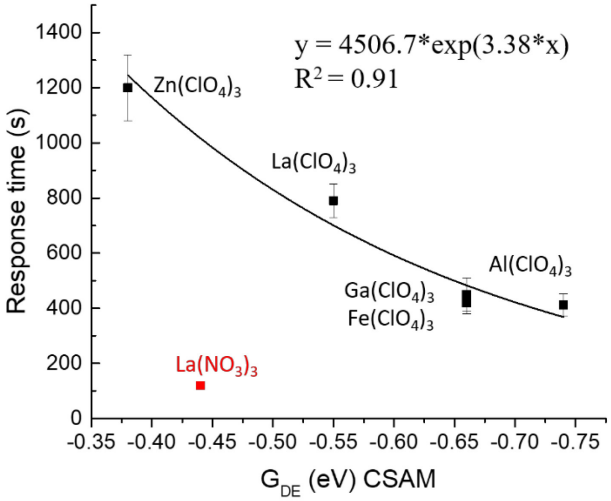

Figure S7. Experimental response time of 5CB anchored to various metal salts upon exposure to DMMP as a function of the calculated G_{DE} using CSAM. Exponential curve fitted using only perchlorate salt results.

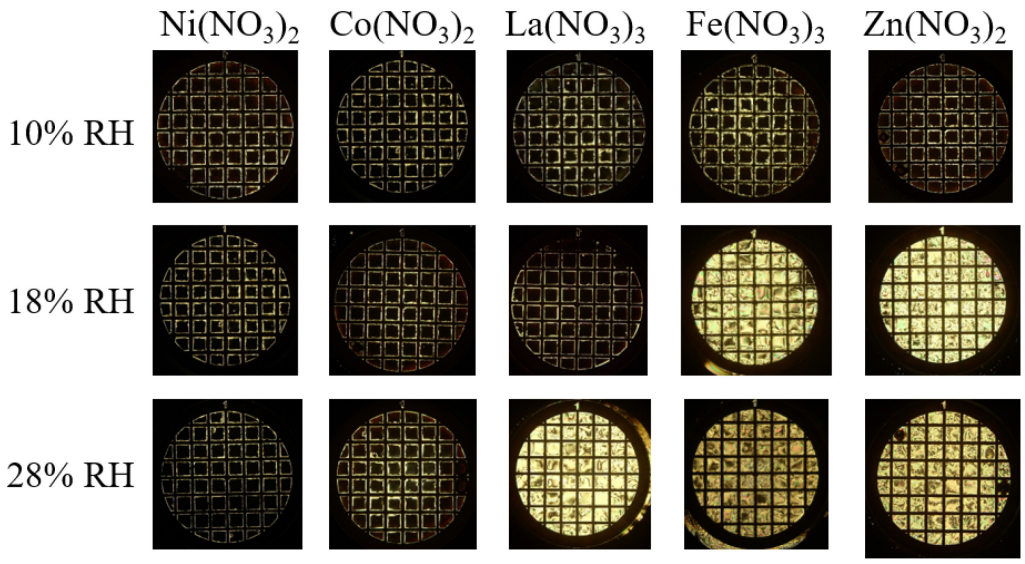

Figure S8. Cross-polarized images of 5CB films on the metal nitrate salts-decorated glasses in the experiment setup a in Figure 2 The samples were made in three separate days with ambient humidity of 10%, 18% and 28% RH.

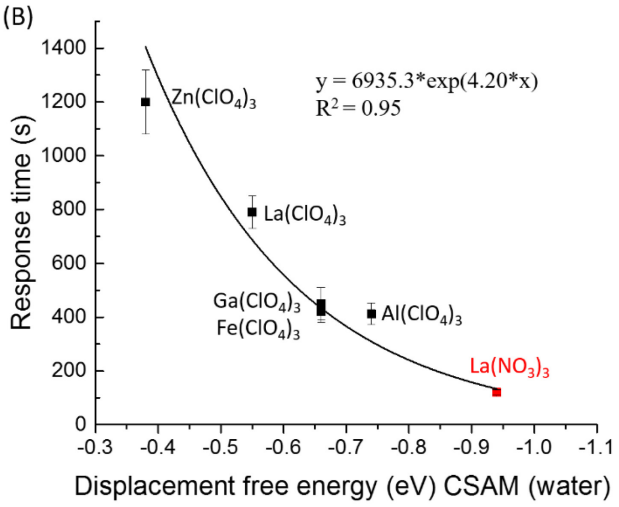

Figure S9. Experimental response time of 5CB anchored to various metal salts upon exposure to DMMP as a function of the calculated G_{DE}. Exponential curve fitted using all metal salt results after correction using water correction on $La(NO_3)_3$.